Multi-stack insulator to minimise threshold voltage drift in ZnO FET sensors operating in ionic solutions

J.D. Akrofi, M. Ebert, J.D. Reynolds, K. Sun, R. Hu, M.R.R. de Planque, H.M.H. Chong

PII: S0167-9317(20)30136-2

DOI: https://doi.org/10.1016/j.mee.2020.111348

Reference: MEE 111348

To appear in: *Microelectronic Engineering*

Received date: 4 April 2020

Revised date: 11 May 2020

Accepted date: 12 May 2020

Please cite this article as: J.D. Akrofi, M. Ebert, J.D. Reynolds, et al., Multi-stack insulator to minimise threshold voltage drift in ZnO FET sensors operating in ionic solutions, *Microelectronic Engineering* (2019), https://doi.org/10.1016/j.mee.2020.111348

Multi-stack insulator to minimise threshold voltage drift in ZnO FET sensors operating in ionic solutions

J.D. Akrofi, M. Ebert, J.D. Reynolds, K. Sun, R. Hu, M.R.R. de Planque, H.M.H. Chong

jda1u17@soton.ac.uk

Faculty of Engineering and Physical Sciences

University of Southamptom

May 11, 2020

Abstract

FET biosensors operating in an electrolyte experience a monotonic, temporal and relatively slow change in threshold voltage caused by the hydration of the insulator layer between the electrolyte and the FET's channel. Minimising this temporal change in threshold voltage is critical as, over time, the drain current of n-channel FETs decreases, making it difficult to distinguish between the signal generated in response to analyte - receptor binding events and the background noise generated by the electrolyte and the FET biosensor. While Rapid Thermal Annealing of the insulator layer is known to diminish threshold voltage drift and its negative effects, it is not compatible with a low temperature fabrication process of 200°C. Our low temperature approach to minimising threshold voltage drift involves depositing a tri-layer insulator stack, consisting of a layer of HfO_2 between two Al_2O_3 layers. Wetting ZnO NWFETs with PBS (10 mM phosphate, 150 mM KCl, pH7.4) for an hour, showed that ZnO NWFETs with a stack insulator layer experienced a much smaller threshold voltage and drain current drift (100 mV, 0.064 nA) than ZnO NWFETs with a single material insulator layer ($\geq$ 4300mV, 2.72 nA), Aluminium oxide in this case. Having established the resilience enhancing properties of the stack insulator layer on FETs operating in electrolytes of physiological relevant ionic concentrations; ZnO NWFETs with a stack insulator layer were shown to be capable of detecting the presence of the miDNA-21 strands. This, in effect, paves the way for miRNA sensing experiments in the near future and for exploring the potential of ZnO NWFETs as a diagnostic tool.

Keywords: Field Effect Transistor biosensors; Zinc Oxide Nanowire Field Effect transistor; stack insulator layer; Threshold voltage drift; Phosphate Buffer Solutions; microDNA

1 Introduction

The duration of binding events between analyte and receptors at the surface of a FET biosensor (bioFET) can last anywhere from a few seconds to thousands of seconds. The length of time depends on a number factors including the ionic strength of the surrounding solution; the concentration of analyte in solution; the binding affinity of the analyte to the receptors at the surface; and the mechanism by which the analyte is delivered to the surface of the bioFET [1]. It is, therefore, imperative that bioFETs can operate stably in solution for long periods of time (i.e. $\geq$ 1000 seconds) in order to register the response associated with analyte - receptor binding events.

When bioFETs come into contact with an aqueous solution during the course of a biosensing experiment, they experience a monotonic, temporal and relatively slow change in threshold voltage commonly referred to as drift. This change in threshold voltage is not caused by the analyte or by variations in the electrolyte composition but, in large part, by the hydration of the gate insulator layer between the electrolyte and the bioFET's channel [2]. During hydration, bonds are formed between OH groups in water and the metal/metalloid atoms in the gate insulator [3] such as SiO_2, Si_3N_4, Al_2O_3 and Ta_2O_5, with the reaction being facilitated by the presence of traps and buried surface sites in the insulator. Jamasb et al [4] modelled the growth of a thin, hydrated layer at the surface of the insulator limited by the dispersive transport of water molecules; and showed, theoretically and by experimentation, that the temporal growth of this hydrated layer reduces the effective capacitance of the gate insulator. This reduction occurs because the hydrated section of the insulator layer has a smaller dielectric constant than the underlying, unmodified, insulator layer which also decreases in thickness as, over time, the hydrated layer grows. Consequently, the effective capacitance of the insulator, calculated as the capacitance of the hydrated layer in series with the thinner underlying, unmodified, insulator layer decreases as the hydrated layer grows.

Typically, for n-channel bioFETs a decreasing insulator capacitance would lead to a positive voltage drift. That is to say, over time, the threshold voltage would increase leading to a decrease in the output drain current. Not only does a decreasing output drain current, resulting from threshold voltage drift, dampen any change in current associated with analyte - receptor binding events; it makes it difficult to distinguish between the signal generated by the binding event and the background noise generated by the electrolyte and the bioFET itself. Due to the

variance in the duration of binding events (i.e. a few seconds to thousands of seconds) between analyte and receptors, it is of critical importance that the magnitude of threshold voltage drift is kept to a minimum so as to minimise the negative effects of a diminishing drain current on the function of bioFETs.

Mitigating the effects of threshold voltage drift by the Rapid Thermal Annealing (RTA) of the insulator layer, which reduces the density of hydration facilitating defects such as buried surface sites and traps, has been shown to be quite effective [5] [6]. However, RTA is not a viable option when employing a low temperature fabrication process of 200 °C [7]. This paper presents a low temperature approach to mitigating threshold voltage drift which is centered around depositing a multi-material stack of high-κ dielectric insulators via Plasma Enhanced Atomic Layer Deposition (PEALD). As opposed to the current bioFET design and fabrication standard, which is to deposit a single material high-κ dielectric insulator layer, a stack of appropriately chosen high-κ dielectric insulators will have a larger effective capacitance making it a more potent transducer [8]. More importantly, the effects of hydration are less pronounced on the stack than the single material insulator layer. This is because the change in the effective capacitance, resulting from of the presence of the hydrated layer, is smaller for the stack than for the single material insulator layer where, the effective capacitance is calculated as the capacitance of the hydrated layer in series with the underlying, unmodified, insulator layers. As a result, the bioFET with a stack insulator will experience a smaller threshold voltage drift and drain current shift than the bioFET with a single material insulator layer.

2 Fabrication and Experimentation

To demonstrate this phenomenon, a novel dry etch lift off technique [9] was used to fabricate two devices comprised of 512 Zinc Oxide (ZnO) Nanowire Field effect transistor (NWFETs) arrays (Figure 1(a)) at 150 °C. ZnO in its wurtzite form is naturally a n-type semiconductor [10] and it has a large and direct band-gap (3.37 eV [11]) making it an attractive material for electronic applications. Its large band-gap gives this material the ability to sustain large electric fields and withstand higher breakdown voltages, while enabling lower noise generation, and high temperature and power operation [12]. Using PEALD, a stack insulator layer consisting of 4 nm of HfO_2 between two 8 nm Al_2O_3 layers was deposited on one device Figure 1(c); 24 nm of Al_2O_3

was deposited on the other device 1(d) to be used as a control device. For all Al_2O_3 depositions the substrate was heated to 150°C and 200°C for HfO_2 deposition. Although HfO_2 has a much larger dielectric constant than Al_2O_3 [13] it does suffer from non-ideal effects namely, hysteresis phenomenon [14]. Al_2O_3 has been shown to have a stronger resistance to these non-ideal effects [15] than HfO_2 and is also known to be more compatible with 3-Aminopropyltriethoxysilane (APTES), a commonly used cross linker molecule, thus a greater number of biomolecules can be immobilised at the surface of an Al_2O_3 insulator than a HfO_2 insulator [16]. It is for these reasons that Al_2O_3 was used as the single material insulator layer and the sandwich configuration was adopted for the stack insulator layer, in order to minimise the amount of HfO_2 used.

Figure 1: (a) An optical image of a chip consisting of 512 ZnO NWFET arrays with gate lengths of 20 μm, 30 μm, 40 μm, 60 μm and 90 μm. A NWFET array with a 20 μm gate was used in each of the experiments reported in this paper. (b) Top view scanning electron micrograph of the NWFETs. (c) Schematic of the cross section of the NWFET with a stack insulator layer. (d) Schematic of the cross section of the NWFET with an Al_2O_3 insulator layer.

Figure 2: (a) An image of ZnO NWFETs underneath a sheet of PMMA laser cut to form channels through which to flow PBS from a syringe to wet the surface of the NWFETs. The width of the channels is 1.18 mm. (b) The protocol for the experiment investigating the threshold voltage drift mitigating effects of the stack insulator layer. Both the ZnO NWFETs with the stack insulator layer and the ZnO NWFETs with the Al_2O_3 insulator layer underwent this protocol. (c) The experimental protocol for the proof of concept miDNA sensing investigation.

To investigate whether ZnO NWFETs with a stack insulator layer have a lower hydration related threshold voltage drift than ZnO NWFETs with a single material (Al_2O_3) insulator layer; Phosphate Buffered Solution (PBS) (10 mM phosphate, 150 mM KCl, pH 7.4) was delivered to the surface of each device through laser cut poly methyl methacrylate (PMMA) microfluidic channels Figure 2(a). The ionic strength of the PBS used in this experiment was made up to 150 mM (Debye length of 0.7 nm) because the ionic strength of most physiological samples is $\geq$ 100 mM [17], [18], [19]. I_DV_G sweeps were recorded before and after both devices were wetted with PBS, in dry conditions. In the subsequent hour, while each device was wetted with PBS, the drain current was

recorded. For this current-time wet measurement, both devices were biased in the subthreshold region with a gate voltage of 4 V and a drain voltage of 2 V. The devices were biased in the subthreshold region as it has been shown to be the most sensitive region of bioFET operation for concentration related sensing [20]. That is to say, bioFETs are most sensitive to changes in analyte concentration when operating in this region; and as these are the kinds of future sensing experiments we aim to be conducting, biasing in the subthreshold region was deemed to be expedient. Moreover it enables the NWFETs to be employed as low power devices.

Following the investigation into the drift minimising effects of the stack insulator layer, a proof of concept experiment was implemented to demonstrate the potential of ZnO NWFETs with a stack insulator layer as a biosensing tool. microDNA (miDNA) are the stable biological equivalent of microRNA (miRNA). miRNA are an important group of non-protein coding RNA molecules which regulate gene expression at the transcriptional and post-transcriptional level in wide range of animals, plants, and viruses [21]. The down-regulation of miRNA is observed in a wide variety of cancers. As such, miRNA profiles can be used to deduce the developmental lineage and differentiation states of tumours [22], making miRNA a vital group of cancer diagnostic biomarkers. As miRNA are unstable molecules (i.e. degrade easily), equivalent microDNA (miDNA) strands are used in most proof of concept experiments to demonstrate the ability of a device to detect miRNA [23]. The analyte used in this experiment was 100 nM of miDNA-21 in Trisma-EDTA (TE) Buffer (20 μ M Trizma, 100 μ M KCl, 2 μ M EDTA). This buffer solution had a Debye length of, approximately, 30 nm. The protocol pictured in Figure 2(c) describes how the experiment was conducted.

A fresh device also consisting of 512 ZnO NWFET array with a stack insulator layer was used for this experiment. This device was also biased in the subthreshold region however, in this instance, with a gate voltage of 1.2 V and a drain voltage of 3 V. Although this device was identical to the ones used in the previous experiments, its $I_D V_G$ characteristic were slightly different hence the different bias voltages. All electrical measurements were conducted in a dark environment, at room temperature, using the Keysight Semiconductor Parameter Analyzer (B1500A). It is important to note that all drain current - time measurements involving buffer solution without miDNA-21 are control measurements and that the reason for allowing the buffer solution to evaporate was to ensure that the strands of miDNA-21 physisored to the surface of the stack insulator layer. This was done in the absence of a functionalisation step which would have,

unnecessarily, prolonged this proof of concept experiment.

3 Results & Discussion

Figure 3(a) shows I_DV_G curves for both devices in dry conditions. As mentioned above, the bias voltages chosen for both devices were a gate voltage of 4 V and a drain voltage of 2 V. The data generated from the I_DV_G sweeps in Figure 3(a) showed that these bias voltages produced a 1.40 nA current for the ZnO NWFETs with the stack insulator and 2.79 nA current for ZnO NWFETs with the Al_2O_3 insulator. Figure 3(b) depicts how the drain current of each device varies over an hour when wetted with PBS. In comparing the drain current before and an hour after PBS was initially delivered to the surfaces of both devices, it was seen that the drain current of the ZnO NWFETs with the Al_2O_3 insulator had shifted by 2.72 nA to a value of 73.8 pA (left axis of Figure 3(b)) by the end of the experiment. Although the drain current of this device exhibited some stability over the course of the experiment (i.e. drain current varied by, roughly, 2 pA during the experiment), the magnitude of the drain current of this device was in the range of the leakage current. Hydration causing a bioFET to drift into the range of leakage current is detrimental to its function as biosensor, as negatively charged analyte such as DNA would have the effect on n-channel bioFETs of decreasing the drain current. Consequently, any change in current associated with an analyte-receptor binding event will be virtually indistinguishable from the leakage current, thus rendering such a bioFET effectively useless.

Figure 3: (a) I_DV_G curves of the ZnO NWFETs before they were wetted with PBS (step 1 in Figure 2(b)). (INSET) I_DV_G curves of the ZnO NWFETs after being wetted with PBS (step 5 in Figure 2(b)). (b) Drain Current against Time graph for NWFETs while wetted with PBS (step 3 in Figure 2(b)). Both devices were biased with in the subthreshold region (gate = 4 V; drain= 2 V) where each is producing nano Amp currents an order of magnitude above the leakage current. The time resolution is 60s for each curve, with both curves showing a slight increase in current as they stabilise over the course of the experiment.

Figure 4: (a) Drain Current against Time graph for ZnO NWFETs with a stack insulator in TE Buffer and then in a solution of TE Buffer with 100 nM miDNA-21 (steps 2 and 9 in Figure 2(c)).

(b) Drain Current against Time graph of the NWFETs in rehydrated TE Buffer and then in a rehydrated solution of TE Buffer with 100 nM miDNA-21 (steps 5 and 13 in Figure 2(c)). Both graphs (a) and (b) show fluctuations in the signal which might be due to miDNA strands detaching then reattaching to surface of the ZnO NWFETs. (c) Drain Current against Time graph for NWFETs obtained after TE Buffer was allowed to evaporate (steps 4 and 11 in Figure 2(c)).

As seen in the I_DV_G sweep of the same device, taken after the wet measurement Figure 3(a) (inset), the drain and leakage currents of this device have both increased by two orders of magnitude. Furthermore, the drain current is yet to reach saturation even at a gate voltage of 10 V, indicating that the devices has not switched on by this point. That is to say, the threshold voltage the ZnO NWFETs with Al_2O_3 insulator layer is greater than 10 V. Given that the threshold voltage of this device, calculated using the 2^{nd} derivative method [24], was 5.7 V before it was wetted with PBS for an hour; we estimate the threshold voltage to have shifted by least 4300 mV over the duration of the wet measurement. To summarise, it is seen that the over course of an hour, the drain current and threshold voltage of the ZnO NWFETs with the Al_2O_3 insulator layer shifts by 2.72 nA and $\geq$ 4300 mV, respectively, when wetted with PBS.

The ZnO NWFETs with the stack insulator layer, in stark contrast, produced a significantly smaller change in drain current of 0.064 nA. This corresponded to a 100 mV threshold voltage drift over the course of the hour long investigation. During this period the drain current of this device showed quite remarkable stability as it only varied by 0.04 nA. Furthermore, the output current was 2 orders of magnitude above the leakage current range, thus eliminating any potential difficulties in differentiating between the leakage current and the output signal generated in response to an analyte-receptor binding event at the surface of NWFETs. The I_DV_G sweep of the ZnO NWFETs with the stack layer taken after the wet measurement Figure 3(a) (inset), shows a devices which is still in working condition. Compared with the noisy I_DV_G sweep of the barely functioning ZnO NWFETs with the Al_2O_3 layer, it emphasizes the enhanced protection against the detrimental effects of hydration that the stack insulator layer provides.

Table 1 summarises the results obtained which support the assertions made above. It was posited that while the insulator layers of both devices would be subject to hydration as a result of being wetted with an electrolyte; the reduction in effective capacitance of the stack insulator layer would be less than reduction in the capacitance of the single material Al_2O_3 insulator layer.

Consequently, the ZnO NWFETs with the stack layer would experience a smaller drift in threshold voltage and drain current than the ZnO NWFETs with the Al_2O_3 layer. The results in Table 1 also show that the ZnO NWFETs with the Al_2O_3 insulator layer experienced a threshold drift rate of 71.7 mV per minute which is of the same order of magnitude as measured bioFET responses [25], [26]. This large threshold voltage drift rate is indicative of a rapidly deteriorating device which, during a biosensing experiment, will drown the response generated by binding events between analyte and receptors. It is even conceivable that such a device might not even register a response especially in cases where the analyte concentration is low as binding events take much longer to occur in such instances. On the other hand, the ZnO NWFETs with the stack insulator layer was observed to have threshold voltage drift rate which was order of magnitude smaller than that observed for ZnO NWFETs with the Al_2O_3 layer. This indicates that the ZnO NWFETs with the stack layer would be able to produce a much more stable response over a longer period of time. The results obtained confirm that the stack layer enhances the resilience of ZnO NWFETs biosensors, operating in electrolytes of physiologically relevant ionic concentrations, by minimising the drift in threshold voltage and drain current.

Table 1: A summary of the experimental results obtained.

Devices	Magnitude of shift in drain current (nA)	Magnitude of threshold voltage drift (mV)	Threshold voltage drift rate (mV/min)
Al_2O_3\ HfO_2\ Al_2O_3 (Stack)	0.004	100	1.67
Al_2O_3	2.72	≥ 4300	71.7

The results obtained from the miDNA sensing experiment show a marked difference between the signal produced by the buffer solution and the signal produced by the miDNA in the buffer solution, in all drain current - time measurement phases of the investigation. The electric field of the negative charge on the miDNA strands, which physisorbed to the surface of the stack insulator, biases the ZnO NWFETs and causes its drain current to decrease as seen in Figure 4. There was at most a 27 nA and a 36 nA difference between the output signals shown in Figure 4(a) and Figure 4(b), respectively, over the course of the measurement. This difference was most pronounced when comparing output currents when the buffer solution is evaporated Figure 4(c).

There was at least a 78 nA difference between the signal produced by the evaporated buffer and signal produced by evaporated buffer with miDNA-21 over a 7200 second period, which was caused by the presence of miDNA strands. It should be noted that rehydration was a precautionary measure taken to identify if the evaporation of the buffer caused an aberration in the output signals (signals overlapping) or whether they followed the same trend as seen with the other measurements.

These results demonstrate the potential of the ZnO NWFETs with stack insulator as a bioFET. Moreover, the minimal threshold voltage drift and drain current shift seen in the previous investigation highlights the enhanced stability the stack insulator gives the ZnO NWFETs, and this will be extremely beneficial in future biosensing applications. While a number of bioFET sensing experiments report contrived output metrics such as percentage change in conductance and normalized responses [25] [27] [28], probably due to the lack of a strong, stable and distinguishable output drain current; the ZnO NWFETs with a stack insulator used in these experiments do not experience any of these issues and as such, one can easily follow how the raw output signal (drain current) varies during an experiment without needing to process the output signal. This will, in the long run, make it considerably easier for non-technical end users to use these bioFETs.

4 Conclusions

BioFETs operating in an electrolyte experience a monotonic, temporal, and relatively slow drift in threshold voltage caused by the hydration of the insulator layer between the electrolyte and the bioFET's channel. It is imperative to the function of bioFETs that drift inducing effects of hydration are minimised as it results in a diminishing drain current. This makes it increasingly difficult to distinguish between the signal generated in response to analyte - receptor binding events and the background noise generated by the electrolyte and the bioFET itself. It has been shown that a tri-layer insulator stack of high-κ dielectrics compromised of HfO_2 sandwiched between two Al_2O_3 layers experiences drift to lesser degree than a single material insulator layer comprised of Al_2O_3. This is because the stack insulator experiences a smaller, hydration related, change in effective capacitance than the single material insulator layer. Having established the resilience enhancing properties of the stack insulator on ZnO NWFETs operating in electrolytes of

physiological relevant ionic concentrations; ZnO NWFETs with a stack insulator were shown to be capable of detecting the presence of the miDNA-21 strands. These results pave the way for miRNA sensing experiments in the near future and for exploring the potential of the ZnO NWFETs as a diagnostic tool.

We would like to acknowledge the support of the Norman Godinho PhD award and the Southampton Nanofabrication Centre.

Conflict of interest: None

References

[1] Todd M. Squires, Robert J. Messinger, and Scott R. Manalis. "Making it stick: convection, reaction and diffusion in surface-based biosensors". In: *Nature Biotechnology* 26 (Apr. 2008), p. 417. URL: https://doi.org/10.1038/nbt1388.

[2] Luc Bousse and Piet Bergveld. "The role of buried OH sites in the response mechanism of inorganic-gate pH-sensitive ISFETs". In: *Sensors and Actuators* 6.1 (1984), pp. 65–78. ISSN: 0250-6874. DOI: doi.org/10.1016/0250-6874(84)80028-1.

[3] A. Hartstein and D. R. Young. "Identification of electron traps in thermal silicon dioxide films". In: *Applied Physics Letters* 38.8 (1981), pp. 631–633. DOI: 10.1063/1.92459. eprint: https://doi.org/10.1063/1.92459. URL: https://doi.org/10.1063/1.92459.

[4] Shahriar Jamasb, Scott Collins, and Rosemary L. Smith. "A physical model for drift in pH ISFETs". In: *Sensors and Actuators B: Chemical* 49.1 (1998), pp. 146–155. ISSN: 0925-4005. DOI: doi.org/10.1016/S0925-4005(98)00040-9.

[5] Tung-Ming Pan, Chao-Wen Lin, and Min-Hsien Wu. "Development of high-K HoTiO3 sensing membrane for pH detection and glucose biosensing". In: *Sensors and Actuators B: Chemical* 144.1 (2010), pp. 139–145. ISSN: 0925-4005. DOI: doi.org/10.1016/j.snb.2009.10.049.

[6] Tung-Ming Pan, Min-Hsien Wu, and Chao-Sung Lai. "Study of high-k Er2O3 thin layers as ISFET sensitive insulator surface for pH detection". In: *Sensors and Actuators B: Chemical* 138.2 (2009), pp. 619—624. ISSN: 0925-4005. DOI: doi.org/10.1016/j.snb.2009.01.051.

[7] Julien Beynet, Yong-Min Yoo, and Mireille Maenhoudt. "Low temperature plasma-enhanced ALD enables cost-effective spacer defined double patterning (SDDP)". In: *Lithography Asia 2009*. Ed.

by Alek C. Chen et al. Vol. 7520. International Society for Optics and Photonics. SPIE, 2009, pp. 489–495. DOI: 10.1117/12.836979. URL: https://doi.org/10.1117/12.836979.

[8] Bobby Reddy, Muhammad A. Alam, and Rashid Bashir. "High-k dielectric Al2O3 nanowire and nanoplate field effect sensors for improved pH sensing". In: *Biomedical Microdevices* 13.2 (Apr. 2011), pp. 335–344. ISSN: 1572-8781. DOI: 10.1007/s10544-010-9497-z.

[9] M Ebert, M R R de Planque, and H M H Chong. "Multichannel ZnO nanowire field effect transistors by lift-off process". In: *Nanotechnology* 29.41 (2018), p. 415302. DOI: 10.1088/1361-6528/aad4c5. URL: https://doi.org/10.1088%2F1361-6528%2Faad4c5.

[10] A. F. Lotus, D. H. Reneker, and G. G. Chase. "Electrical, structural, and chemical properties of semiconducting metal oxide nanofiber yarns". In: *Journal of Applied Physics* 103.2 (2008), p. 024910. DOI: 10.1063/1.2831362.

[11] A. Ohtomo, H. Koinuma, and M. Kawasaki. "Single crystalline ZnO films grown on lattice-matched ScAlMgO4(0001) substrates". In: *Applied Physics Letters* 75.17 (1999), pp. 2635–2637. DOI: 10.1063/1.125102.

[12] Ü. Özgür, S.-J. Cho, and H. Morkoç. "A comprehensive review of ZnO materials and devices". In: *Journal of Applied Physics* 98.4 (2005), p. 041301. DOI: 10.1063/1.1992666.

[13] Robertson, J. "High dielectric constant oxides". In: *Eur. Phys. J. Appl. Phys.* 28.3 (2004), pp. 265–291. doi: 10.1051/epjap:2004206. URL: https://doi.org/10.1051/epjap:2004206.

[14] Tseng-Fu Lu, Chi-Fong Ai, and Chao-Sung Lai. "Non-ideal effects improvement of SF6 plasma treated hafnium oxide film based on electrolyte-insulator-semiconductor structure for pH-sensor application". In: *Microelectronics Reliability* 50.5 (2010). 2009 International Electron Devices and Materials Symposium (IEDMS), pp. 742–746. ISSN: 0026-2714. DOI: https://doi.org/10.1016/j.microrel.2010.01.029.

[15] M.J. Schöning, Yu.G. Vlasov, and H. Lüth. "Can pulsed laser deposition serve as an advanced technique in fabricating chemical sensors?" In: *Sensors and Actuators B: Chemical* 78.1 (2001). Selected Papers from Eurosensors XIV, pp. 273–278. issn: 0925-4005. DOI: https://doi.org/10.1016/S0925-4005(01)00825-5.

[16] Shih-Hsiang Shen et al. "An enhancement of high-k/oxide stacked dielectric structure for silicon-based multi-nanowire biosensor in cardiac troponin I detection". In: *Sensors and Actuators B: Chemical* 218 (2015), pp. 303–309. ISSN: 0925-4005. DOI: https://doi.org/10.1016/j.snb.2015.05.002.

[17] Roey Elnathan, Raisa Kantaev, and Fernando Patolsky. "Biorecognition Layer Engineering: Overcoming Screening Limitations of Nanowire-Based FET Devices". In: *Nano Letters* 12.10 (2012), pp. 5245–5254. DOI: 10.1021/nl302434w.

[18] Yuri L. Bunimovich et al. "Quantitative Real-Time Measurements of DNA Hybridization with Alkylated Nonoxidized Silicon Nanowires in Electrolyte Solution". In: *Journal of the American Chemical Society* 128.50 (2006), pp. 16323–16331. DOI: 10.1021/ja065923u.

[19] Ayako Oyane et al. "Preparation and assessment of revised simulated body uids". In: *Journal of Biomedical Materials Research Part A* 65A.2 (2003), pp. 188–195. DOI: 10.1002/jbm.a.10482. URL: https://onlinelibrary.wiley.com/doi/abs/10.1002/jbm.a.10482.

[20] Xuan P. A. Gao, Gengfeng Zheng, and Charles M. Lieber. "Subthreshold Regime has the Optimal Sensitivity for Nanowire FET Biosensors". In: *Nano Letters* 10.2 (2010). PMID: 19908823, pp. 547–552. DOI: 10.1021/nl9034219.

[21] Richard M. Graybill and Ryan C. Bailey. "Emerging Biosensing Approaches for microRNA Analysis". In: *Analytical Chemistry* 88.1 (2016), pp. 431–450. DOI: 10.1021/acs.analchem.5b04670.

[22] Jun Lu, H. Robert Horvitz, and Todd R. Golub. "MicroRNA expression profiles classify human cancers". In: *Nature* 435.7043 (2005), pp. 834–838. ISSN: 1476-4687. DOI: 10.1038/nature03702.

[23] Josip Ivica, Philip T. F. Williamson, and Maurits R. R. de Planque. "Salt Gradient Modulation of MicroRNA Translocation through a Biological Nanopore". In: *Analytical Chemistry* 89.17 (2017), pp. 8822–8829. DOI: 10.1021/acs.analchem.7b01246.

[24] Hon-Sum Wong, Thomas J. Krutsick, and Richard V. Booth. "Modeling of transconductance degradation and extraction of threshold voltage in thin oxide MOSFET's". In: *Solid-State Electronics* 30.9 (1987), pp. 953–968. ISSN: 0038-1101. DOI: https://doi.org/10.1016/0038-1101(87)90132-8.

[25] Ning Gao et al. "General Strategy for Biodetection in High Ionic Strength Solutions Using Transistor-Based Nanoelectronic Sensors". In: *Nano Letters* 15.3 (2015), pp. 2143–2148. DOI: 10.1021/acs.nanolett.5b00133.

[26] Luye Mu et al. "Nanoelectronic Platform for Ultrasensitive Detection of Protein Biomarkers in Serum using DNA Amplification". In: *Analytical Chemistry* 89.21 (2017), pp. 11325–11331. DOI: 10.1021/acs.analchem.7b02036.

[27] Vadim Krivitsky, Marina Zverzhinetsky, and Fernando Patolsky. "Antigen-Dissociation from Antibody-Modified Nanotransistor Sensor Arrays as a Direct Biomarker Detection Method in Unprocessed Biosamples". In: *Nano Letters* 16.10 (2016), pp. 6272–6281. DOI: 10.1021/acs.nanolett.6b02584.

[28] Christofer Toumazou et al. "Simultaneous DNA amplification and detection using a pH-sensing semiconductor system". In: *Nature Methods* 10 (June 2013), p. 641.

Highlights

- FET biosensors operating in an electrolyte experience threshold voltage drift
- Voltage drift diminishes the response generated by analyte - receptor binding events
- $Al_2O_3/HfO_2/Al_2O_3$ stack deposited on ZnO nanowires was seen to reduce voltage drift
- Subsequently, ZnO nanowires with a stack were used to detect miDNA-21 strands
- This proof of concept experiment paves the way for future miRNA sensing experiments

Graphical abstract

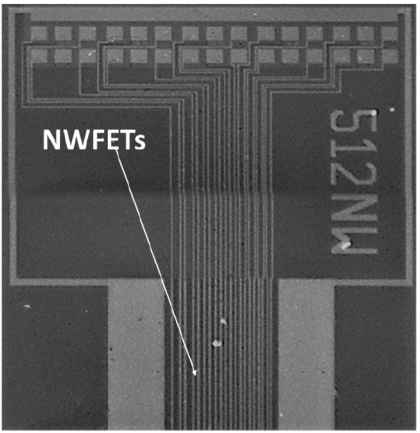

(a)

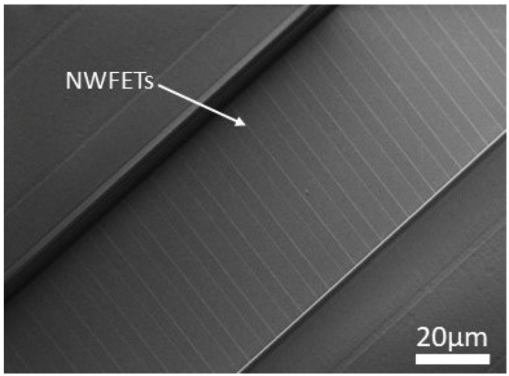

(b)

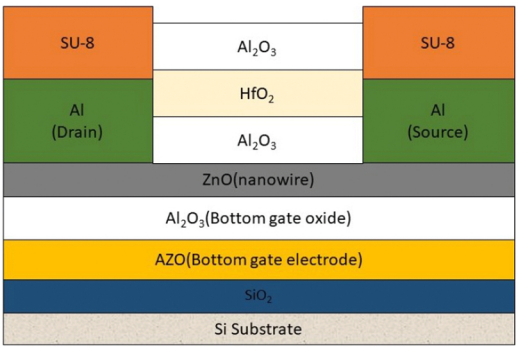

(c)

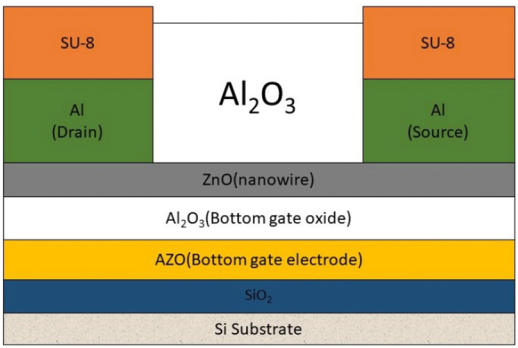

(d)

Figure 1

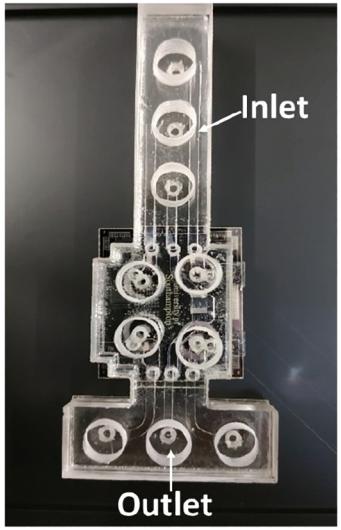
Inlet
Outlet

(a)

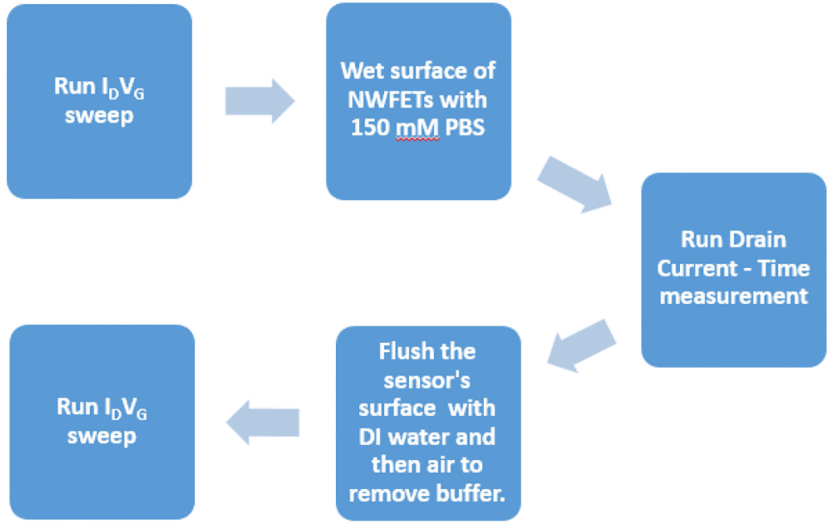
Run I_DV_G sweep
Wet surface of NWFETs with 150 mM PBS
Run Drain Current - Time measurement
Flush the sensor's surface with DI water and then air to remove buffer.
Run I_DV_G sweep

(b)

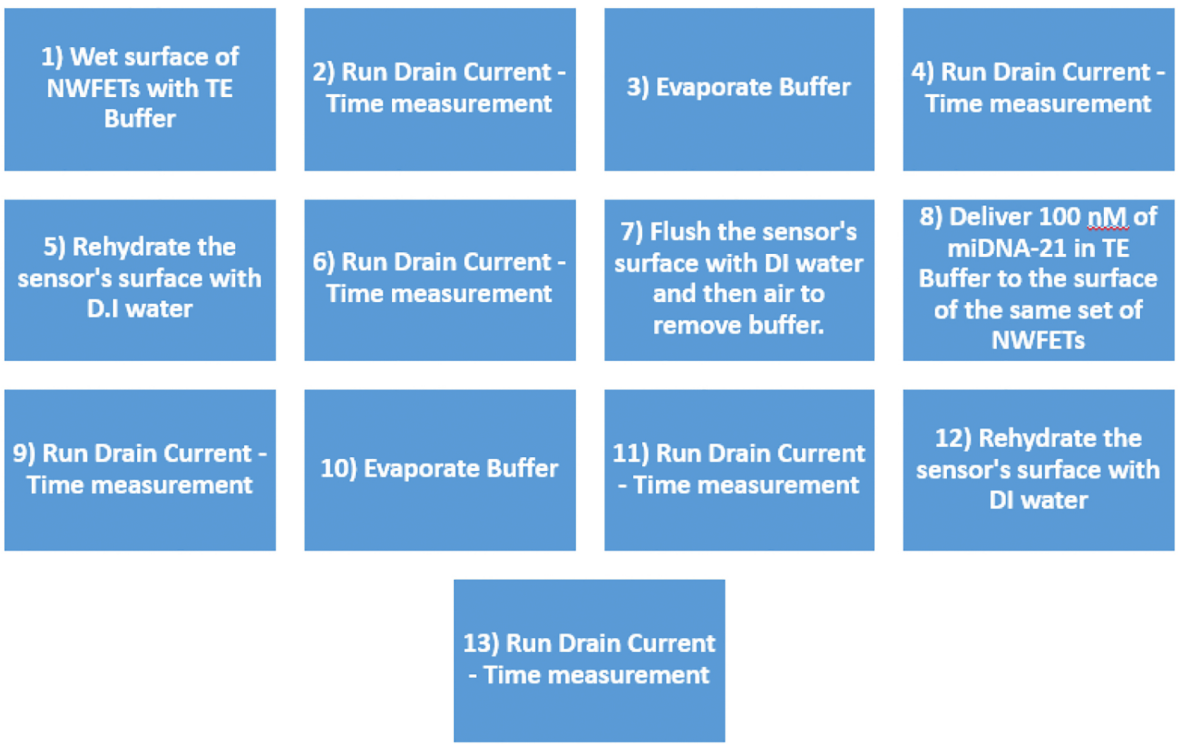
1) Wet surface of NWFETs with TE Buffer
2) Run Drain Current - Time measurement
3) Evaporate Buffer
4) Run Drain Current - Time measurement
5) Rehydrate the sensor's surface with D.I water
6) Run Drain Current - Time measurement
7) Flush the sensor's surface with DI water and then air to remove buffer.
8) Deliver 100 nM of miDNA-21 in TE Buffer to the surface of the same set of NWFETs
9) Run Drain Current - Time measurement
10) Evaporate Buffer
11) Run Drain Current - Time measurement
12) Rehydrate the sensor's surface with DI water
13) Run Drain Current - Time measurement

(c)

Figure 2

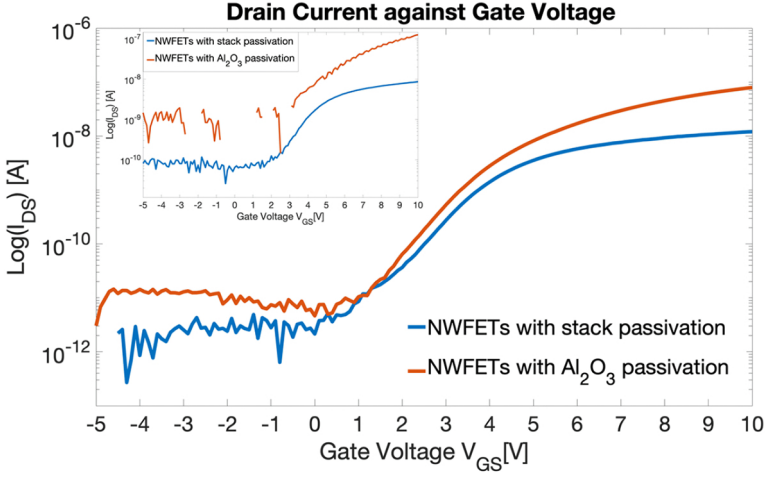
Drain Current against Gate Voltage
NWFETs with stack passivation
NWFETs with Al2O3 passivation
Log(IDS) [A]
Gate Voltage VGS[V]

(a)

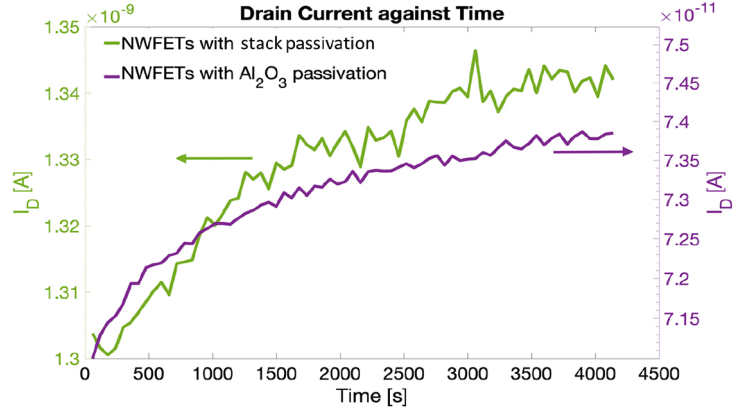
Drain Current against Time
NWFETs with stack passivation
NWFETs with Al2O3 passivation
ID [A]
Time [s]

(b)

Figure 3

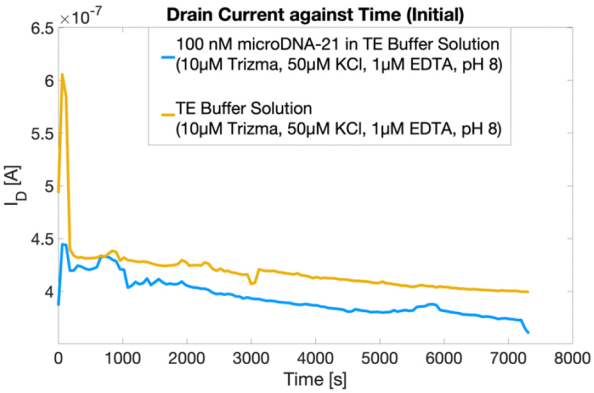
Drain Current against Time (Initial)
×10^-7
100 nM microDNA-21 in TE Buffer Solution
(10μM Trizma, 50μM KCl, 1μM EDTA, pH 8)
TE Buffer Solution
(10μM Trizma, 50μM KCl, 1μM EDTA, pH 8)
I_D [A]
Time [s]

(a)

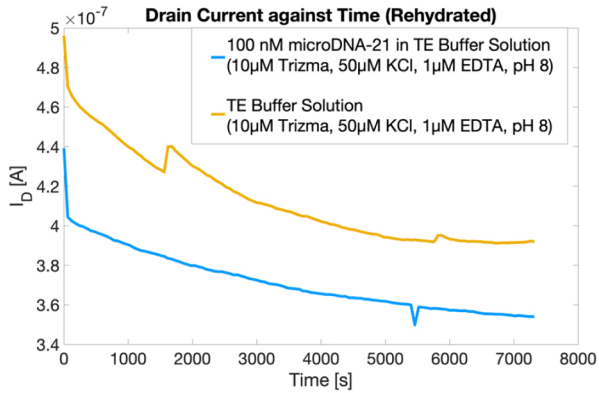
Drain Current against Time (Rehydrated)
×10^-7
100 nM microDNA-21 in TE Buffer Solution
(10μM Trizma, 50μM KCl, 1μM EDTA, pH 8)
TE Buffer Solution
(10μM Trizma, 50μM KCl, 1μM EDTA, pH 8)
I_D [A]
Time [s]

(b)

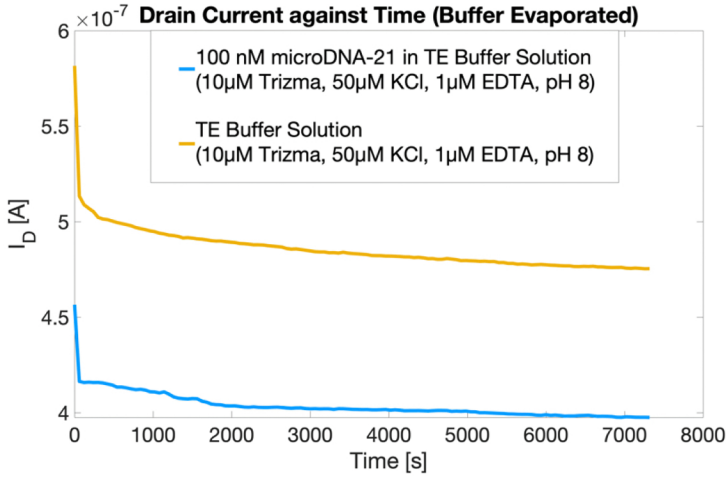
Drain Current against Time (Buffer Evaporated)
×10^-7
100 nM microDNA-21 in TE Buffer Solution
(10μM Trizma, 50μM KCl, 1μM EDTA, pH 8)
TE Buffer Solution
(10μM Trizma, 50μM KCl, 1μM EDTA, pH 8)
I_D [A]
Time [s]

(c)

Figure 4